Analysis of Endoscopic Injectability and Post-Ejection Dripping of Yield Stress Fluids: Laponite, Carbopol and Xanthan Gum

Athira S. Madhavikutty[1], Seiichi Ohta[1,2], Arvind K. Singh Chandel[3], Pan Qi[3] and Taichi Ito[1,3]

[1] *Department of Chemical System Engineering, The University of Tokyo, 7-3-1 Hongo, Bunkyo-ku, Tokyo 113-8656, Japan*
[2] *Institute of Engineering Innovation, The University of Tokyo, 2-11-16 Yayoi, Bunkyo-ku, Tokyo 113-8656, Japan*
[3] *Center for Disease Biology and Integrative Medicine, The University of Tokyo, 7-3-1 Hongo, Bunkyo-ku, Tokyo 113-8655, Japan*

Keywords: Hydrogels, Shear-Thinning, Pressure Drop

Yield stress fluids, which show reversible gel–sol transition and a decrease in viscosity via shear, are expected for endoscopic applications. However, quantitative analyses of such fluids, including pressure drop during endoscopic catheter delivery and post-delivery dripping, have not yet been conducted from a chemical engineering perspective. In this study, we fabricated an equipment setup comprising an endoscopic catheter and a model gastrointestinal (GI) duct to which different concentrations of three model yield stress fluids, specifically, laponite (LAP), Carbopol (CP), and xanthan gum (XG), were applied and compared. We clarified the tradeoff between the pressure drop through the catheter and dripping on the GI duct model. In terms of operability, LAP performed better than CP and XG. The effect of gravity on dripping, which is greatly affected by the position of a patient, was discussed. Finally, the relationship between the operability and rheological properties such as viscosity, yield stress, and restructuring time of the three materials were quantitatively studied.

Introduction

Injectable hydrogels are widely used in medical applications including wound dressing, hemostat, drug delivery, tissue engineering, and bioprinting, among others, owing to their excellent operability and therapeutic efficacy (Ito *et al.*, 2007; Nakagawa *et al.*, 2017). In clinical practice, injectable hydrogels are designed to flow through applicators, such as needles and catheters. They are applied on the surface or inside the targeted tissues or organs where gelation is induced through chemical reactions or physical interactions. To achieve the excellent therapeutic effect of injectable hydrogels, it is generally important to analyze their delivery process in clinical situations in terms of chemical engineering (Ohta *et al.*, 2017; Amano *et al.*, 2018). Although many biocompatible injectable hydrogels (Li *et al.*, 2012) have been reported, there are only a few such studies that explored their operability in clinical settings (Mandal *et al.*, 2020).

Recently, the use of endoscopy, a minimally invasive treatment technique that aids the diagnosis and treatment of gastrointestinal (GI) disorders, has rapidly expanded in the therapeutic field. According to this growth of endoscopy application to meet the rising clinical demand, endoscopically injectable hydrogels have attracted attention for use in endoscopic submucosal dissection (ESD), hemostasis, mucus protection, and wound healing, among others (Onuma *et al.*, 2016). These hydrogels may be pre-formed or precursor liquid-type hydrogels, which form hydrogels at the applied site. Fibrin glue (Rutgeerts *et al.*,1997) is a representative precursor liquid-type hydrogel that has been used in the GI tract for hemostasis and wound dressing (Tsuji *et al.*, 2014) to cover trauma. Contrary to the precursor liquid type, pre-formed hydrogels eliminate the need for in situ cross-linking reactions, for example, using UV, pH, or temperature, and thus show potential for endoscopy. Endoscopic hydrogel delivery requires passage through long channels of various specifications (**Table S1**) to reach the trauma site (Varadarajulu *et al.*, 2011). Typically, the diameter and length of endoscopic channels have ranges of 1.2–4.8 mm and 70–190 cm, respectively. During material delivery, there is a maximum force and a corresponding pressure beyond which the flow resistance is too high for hand injection. In general, viscous or viscoelastic materials such as hydrogels require high pressure for ejection, particularly when the flow channel is long and narrow. Therefore, the pressure drop of hydrogels through endoscopic catheters is an important parameter that limits their clinical application. Thus, hydrogels that exhibit sol-like behavior inside the endoscopic catheter are expected to be easily applied.

Received on March 1, 2021; accepted on May 13, 2021
DOI: 10.1252/jcej.21we018
Correspondence concerning this article should be addressed to T. Ito (E-mail address: taichi@m.u-tokyo.ac.jp).
ORCiD ID of S. Ohta is https://orcid.org/0000-0002-4775-8199
ORCiD ID of A. K. Singh Chandel is https://orcid.org/0000-0002-7130-7734
ORCiD ID of T. Ito is https://orcid.org/0000-0002-1589-8242

Yield stress fluids have the potential for such use because they exhibit a solid-like response at low shear and a solution ("sol")-like response at high shear. Examples of yield stress materials include Carbopol (CP), laponite (LAP), and xanthan gum (XG). CP is a hydrogel microparticle network of poly (acrylic acid) that hydrates and swells in water to form a jammed network (Gutowski *et al.*, 2012). LAP is a colloidal nanoclay gel that constitutes octahedral edges of positively charged magnesium oxide sandwiched between two parallel tetrahedral sheets of negatively charged silica. These oppositely charged faces and edges interact to form a network structure (Becher *et al.*, 2019). Meanwhile, XG is a polysaccharide hydrogel composed of complex aggregates formed through hydrogen bonds and polymer entanglement (Song *et al.*, 2006). Two main reversible interactions that were previously proposed are responsible for the yield stress fluid behavior: jammed repulsive interactions (e.g., CP) and network attractive interactions (e.g., LAP and XG) (Nelson *et al.*, 2019). Owing to their characteristics, yield stress fluids show high shear-thinning, that is, a reduced viscosity at high shear rates, and thus promise decreased pressure-drop and resistance inside the endoscopic catheter. This shear-driven gel–sol transition is advantageous over other driving forces, such as pH, UV, or temperature, because of the process simplicity and reduced process cost.

Furthermore, owing to their shear-thinning property, several yield stress hydrogels have been developed for biomedical applications (Gaharwar *et al.*, 2014). Hyaluronic acid-based catheter-deliverable hydrogels have been used in tissue engineering and myocardial infarction treatment (Steele *et al.*, 2019). In addition, LAP-polysaccharide (i.e., κ-carrageenan, gelatin, and agarose) hydrogels have been designed for hemostasis, endovascular embolization, and 3D printing (Lokhande *et al.*, 2018). However, fewer hydrogels have been examined for use in endoscopic applications. LAP-alginate hydrogel has been examined for formation of a solid cushion inside the polyp via injection to facilitate endoscopic polyp removal (Pang *et al.*, 2019). In addition to submucosal injection (Hirose *et al.*, 2019; Yoshida *et al.*, 2020), the administration of these hydrogels on the surface of trauma or a mucosa layer via endoscopy is increasing for hemostasis, wound protection, and healing. For example, PuraStat, a peptide-based hemostatic hydrogel, has been clinically studied for endoscopic hemostasis (Pioche *et al.*, 2016). Moreover, an epidermal growth factor-containing chitosan hydrogel has been endoscopically delivered for ulcer healing in the stomach (Maeng *et al.*, 2014).

Another issue associated with endoscopic application of a hydrogel on the GI surface, besides the pressure drop, is dripping or flow of the hydrogel from the trauma site, which is different from their submucosal injection. Because of their fluidity, injectable hydrogels often drip away from the applied area after ejection from the endoscopic catheter. As a result, the coverage of the trauma site becomes insufficient, limiting the therapeutic efficiency of the hydrogels. Although surgical techniques such as exsufflation have been reported to mitigate dripping (Pioche *et al.*, 2016), they require additional procedures and operation time.

Therefore, it is indispensable to design hydrogels that are not only injectable but also sufficiently cover the trauma site by preventing dripping. However, although injection resistance and dripping from trauma are jointly encountered problems in endoscopic mucosal application, no quantitative chemical engineering approaches for analysis of these problems have been established.

In this study, we examined the behavior of yield stress hydrogels in a setting that mimics the clinical scenario of endoscopic application (**Figure 1**), that is, flow through endoscopic catheters and post-delivery dripping from the trauma, using a newly proposed equipment model. We measured the injection resistance due to pressure drop inside the model endoscopic catheter, and post-delivery dripping from trauma via drip area in the model GI duct. LAP, CP, and XG were selected as the model yield stress materials. Although

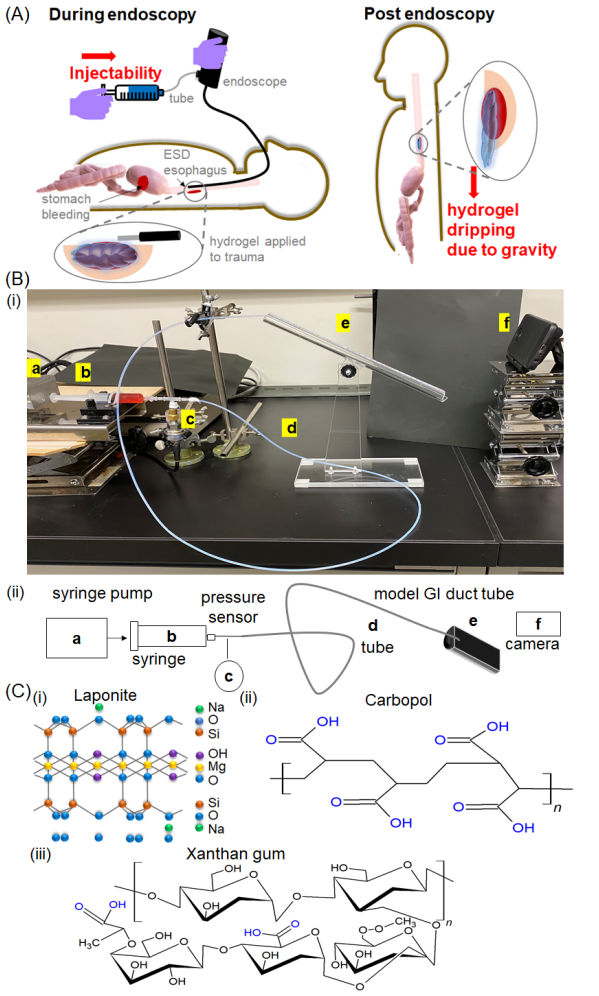

Fig. 1 Description of this research. (A) Endoscopic application of hydrogel for GI treatment. Injection resistance and dripping of hydrogel from trauma site after ejection are two major problems. (B) (i) Photo and (ii) schematic of model catheter and model GI duct for evaluating endoscopic administration of hydrogels in a clinical setting. (C) Chemical structures of model yield stress materials used in this study (i) Laponite (LAP), (ii) Carbopol (CP) and (iii) Xanthan Gum (XG)

these materials have been extensively used in biomedical applications, their potential role in endoscopy has not yet been explored. The obtained pressure drops and drip areas were analyzed based on the rheological properties of the hydrogels.

1. Experimental

1.1 Materials

LAP (XLG-XR) was gifted by BYK Additives and Instruments, XG ($M_W = 2000$ kDa) was donated from Sansho Co., Ltd., and CP (Aqupec HV-805EG, Sumitomo Seika Chemicals Company Limited) was purchased.

1.2 Preparation of hydrogels

LAP powder was added to pure water at concentrations of 2%, 3%, 4%, 5%, and 6% w/v and stirred at 3,000 rpm for 5–6 h. The obtained dispersions were placed at room temperature (25°C) for 60 h to form a stable hydrogel. CP granules were added to pure water at concentrations of 0.5%, 1%, 1.5%, 2%, 2.5%, and 3% w/v and stirred at 1,000 rpm for 12–16 h. The solution was then sonicated in a water bath at 25°C for 20–30 min until the bubbles were removed. XG powder was placed in a beaker, to which pure water was added to prepare 0.5%, 1%, 2%, 3%, and 4% w/v solutions. The XG solutions were stirred for 24 h until uniformity was realized. They were then placed at 25°C for another 12 h to regain any broken polymer bonds.

1.3 Viscoelastic properties of LAP, CP, and XG

A rheometer (MCR302, Anton Paar, Austria) was used to evaluate the viscoelastic properties of the yield stress fluids. The viscosities were measured at shear rates of 10^{-3}–10^{3} s^{-1}. For the measurements, a cone and plate geometry (angle of 1°, diameter of 50 mm, truncation gap of 107 μm) was used to normalize the shear rates across the entire sample (Chen *et al.*, 2017). For all other measurements, a serrated geometry (diameter of 25 mm) was employed. Furthermore, the gel–sol transition was studied via oscillatory amplitude sweep tests at strains of 0.1–200%. The restructuring times of the hydrogels were investigated through alternating low (1%) and high (10%, 100%, 500% and 1,000%) strains. In addition, the yield stress was determined using the oscillatory amplitude sweep results. A liquid trap was employed to prevent solvent evaporation. The temperature of all experiments was set at 25°C for consistency.

1.4 Pressure drop measurement

A model endoscopic catheter tube (**Figure S1**) with the diameter of 2.1 mm and length of 1.8 m (AWG12, PTFE tube, FLON INDUSTRY) was used to measure the pressure drop. Amounts of 8 mL of the solutions were drawn inside a 10-mL syringe (Terumo Corporation), to which the catheter was connected via a commercial plastic fitting kit (731-8228, Female Luer to Female Luer, and 731-8229, Female Luer T-connector, Low-Pressure Fitting Kit; Bio-Rad Laboratories Inc.). The axial velocity was controlled using a syringe pump (ELCM2WF 10 K-AP; maximum thrust force: 80 N, repetitive positioning accuracy: ±0.02 mm; Oriental Motor Co., Ltd.) to establish the volumetric flow rate Q of 10 mL min^{-1}. The pressure drop inside the catheter was measured using a pressure gauge (AP-13S, accuracy: ±5 kPa; Keyence Corp.) at intervals of 100 ms (Hozumi *et al.*, 2015, 2020). The effect of concentration on the pressure drops of LAP, CP and XG was analyzed. We repeated the experiment three times. In addition, the pressure drops of 4 wt% LAP, 2 wt% CP, and 2%w/v XG were measured under the following conditions: flow rates of 5, 10, 15, 20 and 30 mL min^{-1}; catheter diameters of 0.7 and 1.5 mm, and lengths of 0.7, 1, and 2.2 m. The conditions used for the pressure drop measurements are summarized in **Table S2**. Since the materials are injected from syringe through catheter at room temperature (25°C) during endoscopy, we used this temperature condition otherwise stated.

1.5 Drip area measurement

A model GI duct (**Figure S2**) was used to investigate the post-delivery drip areas of the hydrogels. This model is a modified version of the apparatus previously reported for adhesion tests (Rao and Buri, 1989; Khutoryanskiy, 2011). It comprises a semicircular open duct acrylic tube with the diameter of 2 cm and length of 30 cm that is adjustable at various angles. The angle was adjusted horizontally using a digital inclinometer (resolution: ±0.05°; AUTOUTLET, Wanchai, Hong Kong). In endoscopy, the target organs include the esophagus, stomach, and intestine. Therefore, in this study, we fabricated a model GI duct suitable for hydrogel delivery to the esophageal mucosal surface. Two milliliters of the hydrogel flowed out from the endoscopic catheter to the duct. The effect of polymer concentration on the drip area was examined with angles fixed at 45 and 90°. Additionally, the angle was varied at 15, 30, 45, 60, and 90° for 4% w/v LAP, 2% w/v CP, and 2% w/v XG. The flow was observed using a 12 MP, f/1.8 aperture digital camera. The area of the hydrogel that covered the surface was measured after occurrence of the drip, which took less than 10 s following ejection. The width w and length l of the ejected hydrogel were visually measured and used to determine the drip area (assumed to be semicircular, as shown in **Figure S3**) through Eq. (1).

$$A_{\text{drip}} = \text{contact area of gel} = 0.5w\pi \times l \tag{1}$$

2. Results and Discussion

2.1 Measurement of pressure drop: Flow through endoscopic catheter

To initiate the flow through the endoscopic catheter, the hydrogels must undergo a gel–sol transition as a result of the exerted shear. **Figure 2(A)** shows the rheological properties of LAP, CP, and XG as a function of strain. In all cases, the storage modulus G′ decreased with an increase in strain and became lower than the loss modulus G'', at which point the gel–sol transition was considered to occur. The threshold

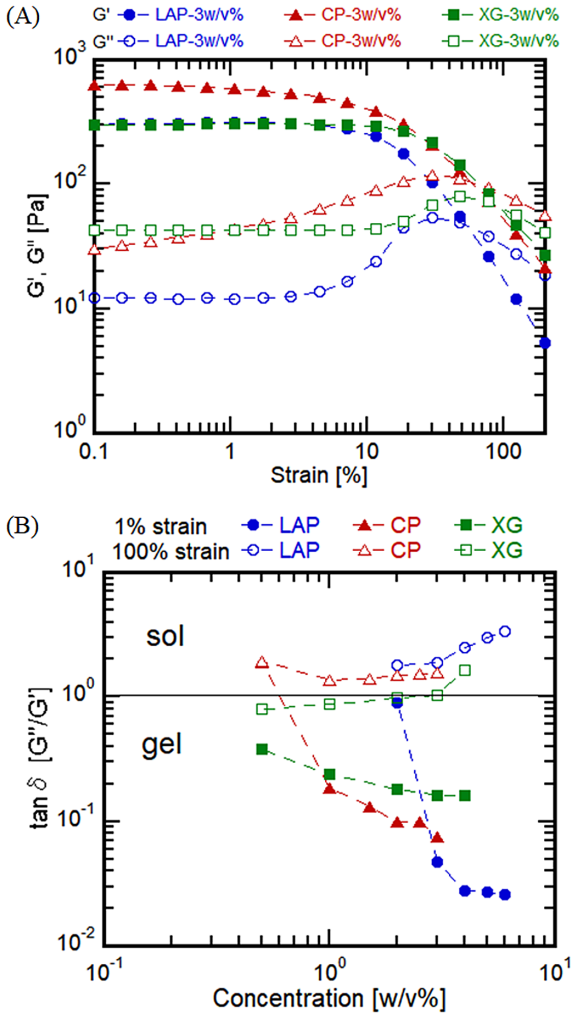

Fig. 2 (A) Strain sweep of 3% w/v LAP, CP and XG (B) Effect of polymer concentration on loss modulus, tan δ at 1% and 100% strain

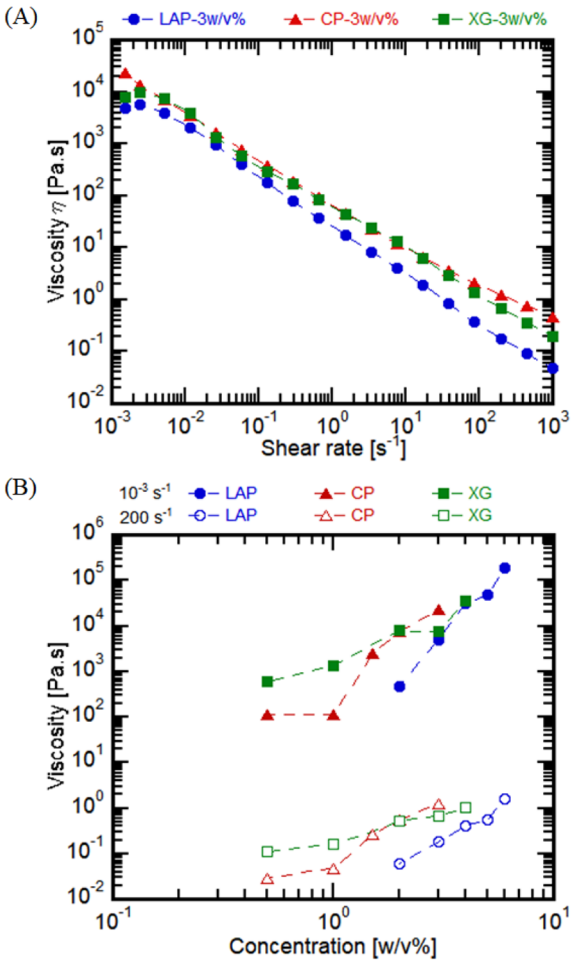

Fig. 3 (A) Flow curves of 3% w/v LAP, CP, and XG. (B) Viscosity results at high (200 s^{-1}) and low (10^{-3} s^{-1}) shear rates and different polymer concentrations

strain of XG at $G' = G''$ (**Figure S4**) was higher than that of LAP and CP because of the long-chain conformation of XG compared with the particle-like conformations of LAP and CP (Nelson and Ewoldt, 2017).

To analyze the data, the loss factor tan δ (i.e., the ratio of G'' to G') was used as a quantifier of viscoelasticity; tan $\delta = 1$ was defined as the gelation point, whereas tan $\delta < 1$ and tan $\delta > 1$ represent the elastic and viscous states, respectively. At 1% strain, the results in **Figure 2(B)** showed that tan $\delta < 1$ for LAP $\geq$2% w/v, CP $\geq$1% w/v, and XG $\geq$0.5% w/v, although lower concentrations (such as 0.5% w/v CP) showed tan $\delta > 1$. On the other hand, at 100% strain, tan δ was greater than one except for 0.5% and 1% w/v XG, indicating the shear-induced gel to solution transition.

After flow initiation inside the endoscopic catheter, the viscosity of the hydrogel becomes an important factor in determining the flow resistance. As shown by the flow curves of LAP, CP, and XG (**Figure 3(A)**), the viscosity decreased with an increase in shear rate owing to their shear-thinning behavior. In addition, the effect of the polymer concentration on the viscosity is shown in **Figure 3(B)**. For this, the shear rate was fixed at 200 s^{-1}, as the shear rate inside the 2.1 mm catheter at 10 mL min^{-1} was estimated to be 183 s^{-1} using Eq. (2),

$$\gamma = \frac{32Q}{\pi D^3} \tag{2}$$

where Q and D represent the flow rate and tube diameter, respectively. Another representative shear rate is 10^{-3} s^{-1}, which is close to the rest condition. The viscosity increased with an increase in concentration at shear rates of 10^{-3} and 200 s^{-1}. Between the shear rates of 10^{-3} and 200 s^{-1}, with an increase in concentration, the viscosities of the solutions decreased by the order of 10^4–10^5 for LAP (2–6% w/v) and 10^3–10^4 for both CP (1–3% w/v) and XG (0.1–4% w/v). At low shear rates, face–edge attractions existed within LAP, which resulted in a network commonly known as a "house of cards" structure. However, the application of high shear broke the structure, leading to a low-viscous dispersion (Dávila and d'Ávila, 2017). Moreover, upon application of shear, the CP-jammed hydrogel exhibited shear thinning due to interparticle motion, leading to a fluid-like behavior (Daly *et al.*, 2020). Finally, the shear thinning of XG was

due to the disaggregation of the network and alignment of individual polymer molecules in the direction of the shear (Norton *et al.*, 1984).

By fitting the data with the power-law model (Eq. (3)), the viscosities at higher shear rates were calculated as:

$$\mu = K\dot{\gamma}^{n-1} \tag{3}$$

where K is a measure of the fluid consistency, and n is a measure of shear thinning. A higher K value indicates a higher viscosity at rest shear, whereas a higher n value indicates a lower shear thinning. The obtained values of K increased while those of n decreased with the increase in concentration, suggesting that the shear-thinning nature increased with the concentration of LAP, CP, and XG (**Figure S5**). During endoscopic application, the materials are injected through a catheter at room temperature (25°C) to the GI tract at body temperature (37°C). The flow curves of 3% w/v LAP, CP, and XG at 37°C demonstrate that the viscosity decreased by approximately 10% (**Figure S6**).

To assess the impacts of changes in the concentration and flow conditions on the injection resistance, we measured the pressure drop during flow inside the endoscopic catheter. **Figure 4(A)** shows the pressure drop profiles of 3% w/v LAP, CP, and XG inside the 2.1 mm catheter. For each material, the pressure drops increased then plateaued as the fluid flowed through the catheter and out, respectively. The dependence of the point at which the pressure drop plateaued on the polymer concentration is shown in **Figure 4(B)** and **Figure S7(A)**. The pressure drops increased with increasing concentration, from 40 kPa at 2% w/v LAP to 700 kPa at 6% w/v LAP, from 57 kPa at 1% w/v CP to 660 kPa at 3% w/v CP, and from 44 kPa at 0.5% w/v XG to 620 kPa at 4% w/v XG. As 4% w/v LAP, 2% w/v CP, and 2% w/v XG showed a similar pressure drop of 200±20 kPa, we used these concentrations as standard conditions for all the experiments that followed, unless otherwise stated.

During the endoscopic application of materials, there is a maximum pressure drop ΔP_{max}, beyond which the flow resistance is too high for hand injection. The maximum hand-injection pressure drop (Wahlberg *et al.*, 2018) can be calculated using Eq. (4),

$$\Delta P_{max} = \frac{F_{max}}{A_{plunger}} \tag{4}$$

where F_{max} and $A_{plunger}$ represent the maximum force for hand injection and the area of the syringe plunger, respectively.

It has been reported that the F_{max} value of a physician's upper limb is approximately 80 N (male: 95.4 N, female: 64.1 N) (Vo *et al.*, 2016). Because we used a syringe with $A_{plunger}$ of 1.2 cm^2 in our experiment, the average ΔP_{max} was calculated to be 667 kPa. Comparing this value with the results in Figure 4(B), the pressure drops exceeded ΔP_{max} in the cases of 6% w/v LAP, 4% w/v XG, and 3% w/v CP.

As shown in **Figure 4(C)**, the pressure drops of LAP, CP, and XG increased with an increase in the flow rate. At 5 mL min^{-1}, the pressure drop of CP was lower than those of LAP and XG. With an increase in flow rate to

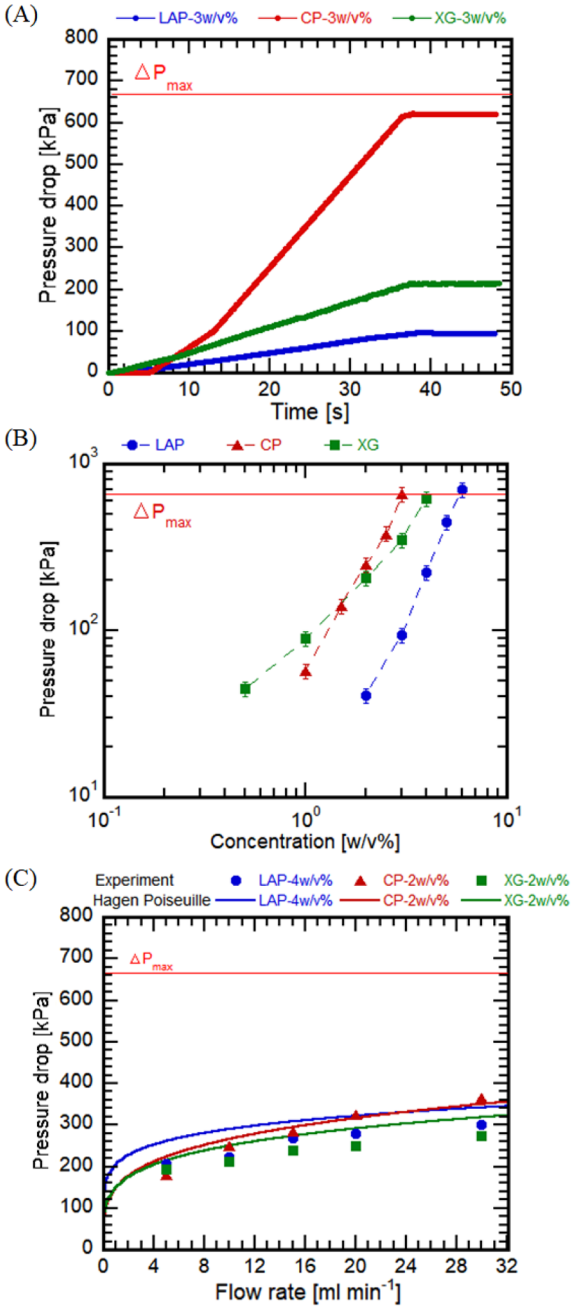

Fig. 4 (A) Time vs. pressure drop for 3 w/v% LAP, CP and XG during the flow through the 2.1 mm endoscopic catheter at 10 mL min^{-1} flow rate; (B) Effect of polymer concentration on the pressure drop at the steady state. ΔP_{max} is the maximum injection pressure drop for hand injection; (C) Effect of flow rate on the pressure drop at steady state. The theoretical lines correspond to the pressure drop predictions by Hagen Poiseuille law for power law fluids (Eq. (5))

10 mL min^{-1}, LAP and XG exhibited lower pressure drops than CP owing to their higher shear-thinning (n_{LAP} = 0.18, n_{XG} = 0.2, n_{CP} = 0.3). We also used the Hagen–Poiseuille law for power-law fluids (Chhabra and Richardson, 1999), given by Eq. (5), to predict the pressure drop ΔP at different flow rates Q inside the catheter of length L and diameter D.

$$\Delta P = \frac{2^{3n+2}\left(\frac{3n+1}{n}\right)^{n} KQ^{n}L}{\pi^{n}D^{n+3}} \quad (5)$$

The K and n values were obtained using Eqs. (2) and (3), respectively, as described previously.

Equation (5) assumes a fully developed laminar flow. The resulting experimental values are comparable to the theoretical predictions. In addition, the pressure drop increased with an increase in length and decreased with an increase in the diameter of the catheter, which was also consistent with the prediction using Eq. (5) (**Figure S7(B)**).

2.2 Measurement of drip area: Quantitative analysis of post-delivery flow behavior

After delivery through the catheter, the hydrogels were expected to undergo a quick sol–gel transition through restructuring of the applied surface. We measured the restructuring of 4% w/v LAP, 2% w/v CP, and 2% w/v XG hydrogels by subjecting them to alternating low (1%) and high (100%) strains. As shown in **Figure 5(A)**, LAP, CP, and XG were gels ($G' > G''$) at low strain, sols ($G'' > G'$) at high strain, and then transitioned again from sol to gel at low strain.

During the restructuring, the sols reformed the broken physical interactions to form hydrogels. The LAP, CP, and XG hydrogels demonstrated the average recovery of 80% in less than 10 s when subjected to strains of 10%, 100%, 500%, and 1,000% (**Figure 5(B)** and **Figure S8**). The quick recovery was due to the reversible attractions and repulsions between particles in the cases of LAP and CP, and the attraction between polymer chains in the case of XG (Nelson *et al.*, 2019). This self-healing behavior due to reversible bonds is advantageous for endoscopy.

Yield stress, which characterizes the onset of hydrogel flow, can be used as a measure of post-delivery drip resistance after restructuring. The hydrogels were subjected to an increased deformation via applied strain between 0.1% and 200%. The yield stress was measured as the shear stress at the limit of the linear viscoelastic region.

The obtained yield stresses of 4% w/v LAP, 2% w/v CP, and 2% w/v XG hydrogels were 88, 15, and 22 Pa, respectively (**Figure 6(A)**). The yield stress increased with increasing

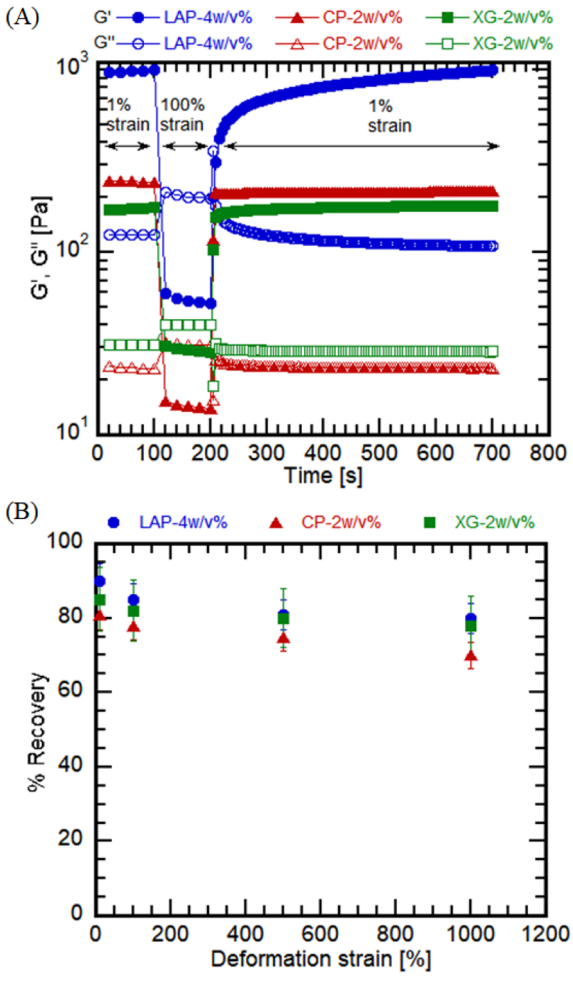

Fig. 5 (A) G' and G'' values of LAP, CP, and XG hydrogels at alternating high (100%) and low (1%) strains (B) Recovery of hydrogels (%) being subjected to different deformation strains (10%, 100%, 500% and 1,000%) for 10 s

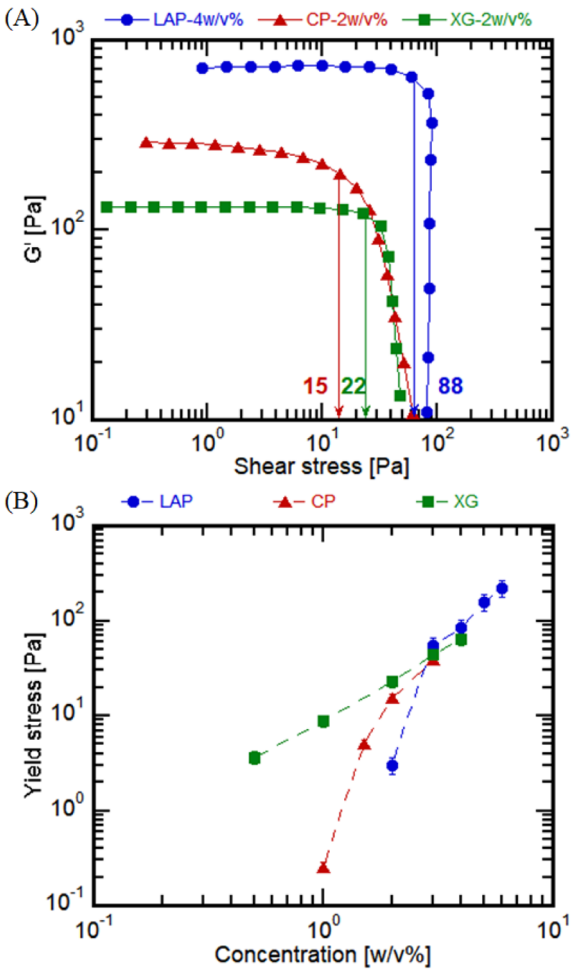

Fig. 6 (A) Amplitude sweep results of 4% w/v LAP, 3% w/v CP and 2% w/v XG (B) Effect of polymer concentration on yield stress of LAP, CP and XG hydrogels

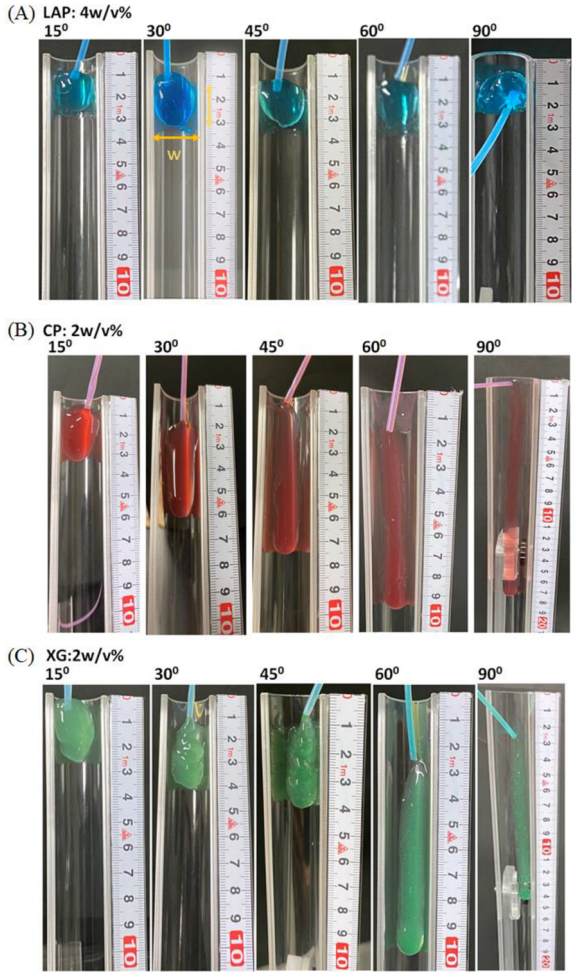

Fig. 7 Images of dripping of hydrogels (A) 4% w/v LAP, (B) 2% w/v CP, (C) 2% w/v XG at different slope angles of the model GI duct tube. The drip areas were obtained using Eq. (1)

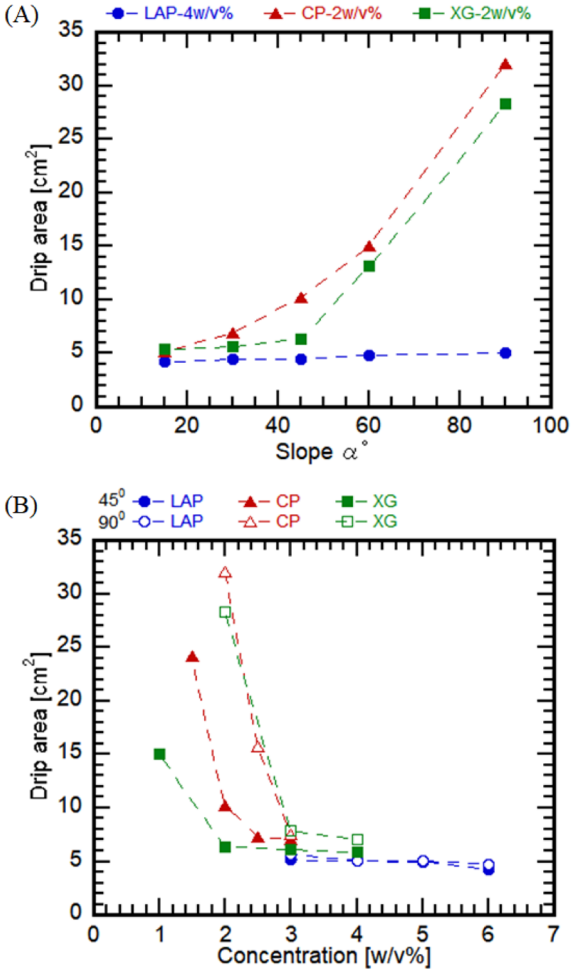

Fig. 8 (A) Effect of slope angle on drip area of 4 w/v% LAP, 2% w/v CP and 2% w/v XG. (B) Effect of polymer concentration on drip area of LAP, CP and XG. The slope angles used are 45° and 90°

concentrations of LAP, CP, and XG (**Figure 6(B)** and **Figure S9**), which could be due to the increased particle or polymer interactions. The mechanism responsible for the yield stress of the materials has been previously investigated in depth (Nelson and Ewoldt, 2017). CP comprises "repulsively interacting, crowded microstructural elements" that are jammed against each other. On the contrary, LAP and XG are "attraction-dominated materials whose microstructures resist being pulled apart." The application of an external shear force rearranges these internal structures to allow the materials to yield and flow.

To analyze the area covered by a hydrogel at the trauma site, we observed the post-delivery dripping on the model semicircular GI duct tube. The drip area on the GI tube was measured using the width and length of the dripped hydrogel 10 s after it was completely ejected from the catheter. In addition, we studied the effect of surface inclination (angle $\alpha = 15$–$90°$) of 4% w/v LAP, 2% w/v CP, and 2% w/v XG hydrogels. Images of the hydrogel drip areas at different slope angles are shown in **Figure 7**.

During treatment, an endoscope is inserted through the mouth of a patient assigned to a lying position. Thus, the inclination angle of the esophageal surface along the direction from the mouth to the stomach of the inserted endoscope is $\alpha = 0°$. However, in cases such as ESD, the hydrogel would be administered on the upper side of the esophageal circumference, such that $\alpha > 90°$. When the patient stands after the treatment, the inclination of the applied hydrogel on the circumference changes to $\alpha = 90°$. As a result, due to the change in the position of the patient, the inclination angle changes dramatically during treatment. Therefore, in this study, α was changed from 15° to 90° in the model GI duct.

We also investigated the effect of the concentrations of LAP, CP, and XG at 45° (**Figure S10**) and 90° (**Figure S11**). As shown in **Figure 8(A)**, with an increase in the slope from 15 to 90°, the drip area remained almost constant for 4% w/v LAP, while it increased by 3 for 2% w/v CP and by 2.5 for 2% w/v XG. At 45°, 2% w/v LAP, 1% w/v CP, and 0.5% w/v XG dripped through the entire length of the duct, and the corresponding drip areas could not be measured. In addition, at 90°, 1.5% w/v CP and 1% w/v XG also dripped through the whole length. As shown in **Figure 8(B)**, with an increase in concentration, the drip area decreased and

gradually plateaued, at which point no dripping was initiated after the ejection.

2.3 Drip area affected by gravity force and yield force

It has been reported that hydrogel flow on an inclined surface is determined using two opposing forces, specifically, the yield force and gravitational force. The ratio of the yield force to the gravitational force (Eq. (6)) is defined as follows:

$$G = \frac{\tau_y A_{\text{drip}}}{mg\sin\alpha} \tag{6}$$

where m is the mass of the hydrogel, τ_y is the yield stress, g is the gravitational acceleration, and α is the inclination angle. If $G > 1$, i.e., the yield force of the hydrogel is high enough to overcome the gravity force; hydrogel dripping would not be initiated, as observed in high concentrations of LAP, CP, and XG (Figure 8(B)).

More specifically, the hydrogel would remain at the ejection site. Meanwhile, if $G < 1$, the gravity force on the hydrogel initiates dripping, which increases A_{drip} and leads to an increase in the yield force. Then, when this increased yield force is balanced with the gravity force ($G = 1$) at a certain A_{drip} value, the dripping would stop. Because the gravity force increases with an increase in the inclination angle α, the drip areas of 2% w/v CP and XG increased. In addition, if the yield force does not exceed the gravity force within the area of the duct tube, the hydrogel would flow out, as observed in 2% w/v LAP, 1% w/v CP, and 0.5% w/v XG at 45°. Moreover, at 90°, the gravity force is even higher, and a greater yield force is required to overcome it, leading to a larger A_{drip} value. Therefore, in addition to the above hydrogel concentrations, 1.5% w/v CP and 1% w/v XG also flowed out. These results suggest that the yield stress, volume, and ejected area of hydrogels, as well as the angle of the applied site, which depends on the patient's position, need to be considered to prevent the dripping of endoscopically applied injectable hydrogels.

2.4 Tradeoff relationship between injectability through the model endoscopic catheter and coverability on the model GI duct of the yield stress fluids

In the previous sections, two major factors for the endoscopic application of injectable hydrogels, specifically, the injectability and trauma coverability, were analyzed using the catheter pressure drop and the post-delivery drip area, respectively. In **Figure 9**, the pressure drop (Figure 4(B)) inside the 2.1 mm catheter at the flow rate of 10 mL min^{-1} (Figure 4(B)) and the drip area (Figure 8(B)) at 45° at different concentrations of the hydrogels are summarized. A tradeoff relationship is apparent; a decrease in the pressure drop resulted in a larger drip area. A lower pressure drop of fluids would be accompanied by higher fluidity, which resulted in their dripping to a wider area.

For clinical application, the pressure drop of the hydrogel needs to be less than ΔP_{max}, while the area covered with the applied hydrogel should correspond to the area of the trauma site, A_{trauma}. These threshold values are shown in Figure 9. Here, it can be observed that for the same pressure drop inside the catheter, the drip area in the case of $\alpha = 90°$ was larger than that at 45° and exceeded A_{trauma} in most cases. In an actual clinical setting, physicians would move the tip of the endoscopic catheter such that the trauma is fully covered. Further, in the case of procedures such as ESD, the entire esophageal circumference is covered. Inclination angle of the equipment corresponds to the patient's position in a clinical situation. For example, the inclination of 90° could relate to the situation when the patient is in a vertical position, i.e., the gravity force on the hydrogel is maximum. Therefore, even if a hydrogel is injectable through an endoscopic catheter, the coverability would be largely affected by the patient's position. By considering the tradeoffs and "white spaces," the materials and process conditions can be optimized for clinical applications as necessary. Although the dripping and distribution of these hydrogels on the transverse plane after ejection needs to be further analyzed in future research, the current study demonstrates their high potential for endoscopy. It can be deduced from these preliminary investigations that the yield stress hydrogels would exhibit good performance in covering trauma sites in clinical scenarios.

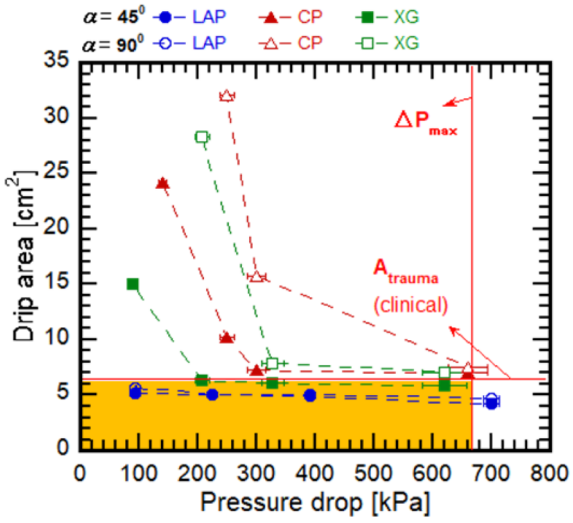

Fig. 9 Relationships between drip area and pressure drop for LAP, CP, and XG at different concentration and at slope angles of 45° and 90°. The 2.1 mm catheter was used for the pressure drop measurements at the flow rate of 10 mL min^{-1}, while the angle of 45° and 90° was used for the drip area measurement. The shaded region represents values ($\Delta P < \Delta P_{\text{max}}$ and $A_{\text{drip}} < A_{\text{trauma}}$) suitable for clinical application

2.5 Rheological properties of yield stress fluids sufficiently predict operability of the yield stress fluids in clinical setting

To understand the tradeoff between the pressure drop and the drip area, we analyzed the hydrogel properties that would affect the flow inside the catheter and post-delivery flow behavior. Using the data obtained for the 2.1 mm catheter at the flow rate of 10 mL min^{-1}, we established the

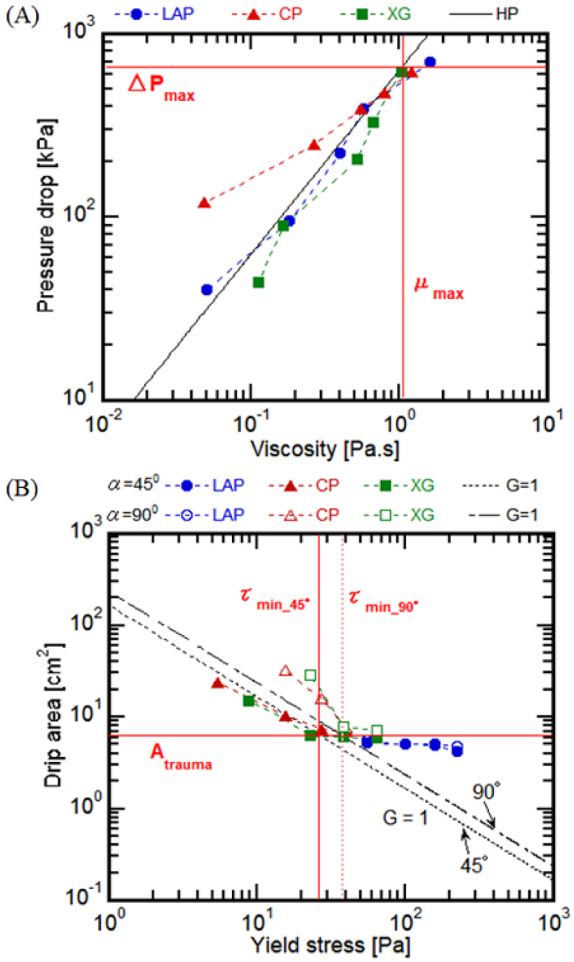

Fig. 10 (A) Pressure drop results of LAP, CP and XG as a function of viscosity inside the 2.1 mm catheter at the flow rate of 10 mL min^{-1}, (B) Drip areas of LAP, CP and XG as a function of yield stress at inclination angles of 45° and 90°

pressure drops of LAP, CP, and XG as a function of viscosity at different concentrations. As a result, the pressure drop increased with an increase in viscosity for the LAP, CP, and XG hydrogels, as shown in **Figure 10(A)**. By assuming Hagen–Poiseuille flow, the maximum viscosity at which the pressure drop becomes less than ΔP_{max} can be estimated using Eq. (7).

$$\mu_{max} = \frac{\pi D^4 \Delta P_{max}}{128 QL} \tag{7}$$

For the above tube specifications and conditions, the value of μ_{max} was determined as 1.06 Pa s.

The drip area was also realized as a function of yield stress, as presented in **Figure 10(B)**, using the data for the inclination angles of 45 and 90°. The drip area decreased with an increase in the yield stress and approached a constant value. This can be explained using Eq. (6), as discussed in section 2.3. The minimum yield stress τ_{min} required to achieve the complete trauma coverage could be estimated by assuming $G = 1$, as follows:

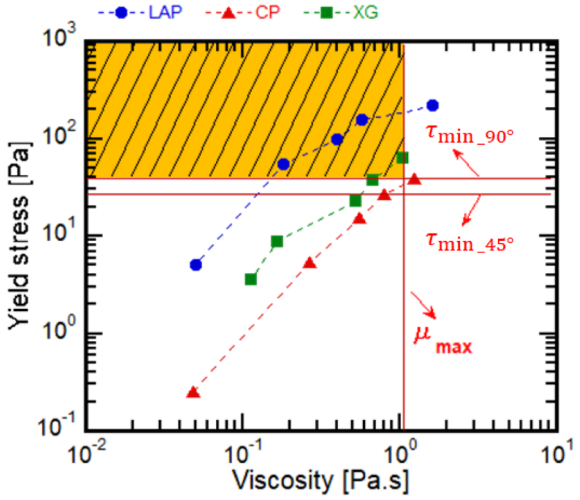

Fig. 11 Results of yield stress and viscosity of LAP, CP and XG hydrogels for the prediction of their endoscopic applicability. The color-shaded region represents $\tau > \tau_{min\_45°}$ and $\mu < \mu_{max}$ while the line-shaded region represents $\tau > \tau_{min\_90°}$ and $\mu < \mu_{max}$

$$\tau_{min} = \frac{V \rho g \sin\alpha}{A_{trauma}} \tag{8}$$

using the values of $A_{trauma} = 6.3\,cm^2$ (Pioche *et al.*, 2016), $g = 9.81\,ms^{-2}$, and assuming $\rho = 1{,}200\,kg\,m^{-3}$, the values of τ_{min} were estimated as 26.42 and 37.37 Pa at 45 and 90°, respectively, from Eq. (8).

Thus, viscosity and yield stress are dominant factors affecting the pressure drop and flow area, respectively, where the former needs to be less than μ_{max} and the latter needs to be higher than τ_{min} to achieve both injectability and coverability, respectively. τ_{min} was found to be higher for a steeper slope, as a higher yield stress would be required to overcome the increased gravity force. Using these relationships, we propose that a "viscosity–yield stress parameter space" similar to that reported in the previous research (Ewoldt *et al.*, 2007) is useful to predict the suitability of injectable hydrogels for endoscopy. The yield stresses of LAP, CP, and XG increased with increasing viscosity (**Figure 11**), which agrees with the relationship between the flow area and pressure drop.

The successful clinical application of the materials is expected if they are chosen from the proposed parameter space (Figure 11), so that both the viscosity and yield stress are within the threshold values. The threshold values μ_{max} and τ_{min} change according to the clinical situation; μ_{max} would change according to the specification of the catheter and flow conditions used, whereas τ_{min} would change with the volume of hydrogel and patient position. By setting the values of μ_{max} and τ_{min} according to the one typical and averaged case of required clinical situations, the proposed viscosity–yield stress parameter space is expected to provide a guide to select the appropriate material condition of injectable hydrogels for endoscopic application without actual measurement of the pressure drop and drip area.

2.6 Usefulness of the concept of the tradeoff relationship between viscosity and yield stress in other medical fields and various industries

Although previous studies have reported the injectability of hydrogels for endoscopic delivery (Yoshida *et al.*, 2020), the coverability of hydrogels applied to the trauma surface has not yet been examined. In addition, although several researchers have deeply explored the material properties of LAP, CP, and XG as yield stress hydrogels (Nelson *et al.*, 2018), their endoscopic application has not yet been analyzed.

Our study was based on the focus that the endoscopic application of hydrogels needs to satisfy both injectability and coverability for clinical applications. Accordingly, we investigated both of these factors simultaneously using a new model equipment setup. We demonstrated the existence of a tradeoff between the pressure drop inside the model endoscopic catheter and the drip area in the model GI duct. We also proposed a simple parameter space for the prediction of pressure drop and drip area using the physical properties of hydrogels, specifically, viscosity and yield stress. Although different grades of materials affect the properties due to changes in molecular weights or particle sizes, in this study, LAP exhibited the best performance among the three fluids. Thus far, these results agree well with those of previous reports. This simple prediction is expected to provide target values for the research and development of new hydrogels for endoscopic applications.

Finally, we noted the limitations of this study. The drip area measurement was conducted using the acrylic model GI tract; thus, the adhesive interaction of hydrogels with the tissue surface was neglected. In addition, although distilled water was used as a solvent for the hydrogels, physiological solutions such as saline or buffer may be used in clinical cases. The pH at the applied site can also differ according to the target trauma site. In addition, the effect of temperature on the rheological properties and function provides insight into the mechanism of yielding of the materials. Future studies on these aspects will contribute to the clinical application of endoscopically injectable hydrogels. Further, integrated studies on the effects of physiochemical interactions and material science on the rheological properties could develop new yield stress materials with improved functionalities.

Owing to the unique and excellent properties of yield stress fluids, they are currently expected for several emerging medical applications such as cell delivery in regenerative medicine and as bio-inks for bio-fabrication in tissue engineering. Such fluids can protect suspended cells from shear, despite the narrow needle of the syringe (Yan *et al.*, 2012). In addition, they enable bio-inks to pass through the narrow nozzle of inkjet printers (Nakagawa *et al.*, 2017) or to be printed directly, known as "direct printing" (Highley *et al.*, 2015), and are utilized for cell culture media to protect cells from shear during rotation culture. In the medical applications, the tradeoff between viscosity and yield stress fluid is potentially important. Thus, the present study suggests the design of hydrogels for these processes. Furthermore, as the yield stress property has been used in several commercial materials such as paints, cement, toothpaste, and mayonnaise, our approach would also be applicable in other industries. For example, industrial 3D printing requires inks that are extrudable and retain their shape after printing (Ribeiro *et al.*, 2017). Another application closely related to our study is the use of emulsions and creams for topical applications. Therefore, the present research would be beneficial for the design of novel yield stress materials for several applications.

Conclusions

In this study, we quantitatively investigated the operability of the three model yield stress hydrogels, LAP, CP, and XG, for endoscopic application. The results indicate that the endoscopic application of the hydrogels depends on their ability to overcome the two resistances, i.e., injection resistance and resistance to drip from trauma. Thus, we used a new equipment setup that can simultaneously measure these two resistances. The two resistances measured through pressure drop and post-delivery drip area, respectively, were found to exhibit tradeoff relationships that depend on the hydrogel concentration. Formulations based on the viscosity and yield stress of the hydrogels were proposed to predict the endoscopic applicability of yield stress fluids without actual measurements of the pressure drop and drip area. This study is expected to clearly demonstrate the target rheological properties for researchers regarding the development of new yield stress fluid materials in endoscopy.

Supplementary Information

Supplementary Information is available at
http://www.scej.org/publication/jcej/suppl/

Acknowledgement

We are grateful to JSPS KAKENHI (Grant-in-Aid for Scientific Research (B); 17H03464, Taichi Ito) for financial support of this work. We thank BYK Additives & Instruments for kindly providing us with the laponite. We also thank Sansho Co., Ltd. for kindly providing us with xanthan gum. We would like to express our gratitude to the Japan International Corporation Agency (JICA) for the scholarship provided to Athira Sreedevi Madhavikutty during her PhD.

Nomenclature

A_{drip}	=	area of dripped hydrogel	[m^2]
A_{trauma}	=	area of patient trauma site	[m^2]
D	=	diameter of catheter	[m]
g	=	acceleration due to gravity	[$m\,s^{-2}$]
L	=	length of catheter	[m]
M_w	=	molecular weight	[Da]
Q	=	average fluid flow rate	[$m^3\,s^{-1}$]
V	=	volume of fluid	[m^3]
α	=	angle of the inclined surface	[°]
ΔP_{max}	=	maximum injection pressure drop	[Pa]
ΔP	=	pressure drop inside tube	[Pa]
μ	=	viscosity of fluid	[Pa s]
ρ	=	density of fluid	[$kg\,m^{-3}$]

τ_y = yield stress of fluid [Pa]
γ = shear rate inside catheter [s^{-1}]

Literature Cited

Amano, Y., Y. Nakagawa, S. Ohta and T. Ito; "Ion-Responsive Fluorescence Resonance Energy Transfer between Grafted Polyacrylic Acid Arms of Star Block Copolymers," *Polymer (Guildf.)*, **137**, 169–172 (2018)

Becher, T. B., C. B. Braga, D. L. Bertuzzi, M. D. Ramos, A. Hassan, F. S. Crespilho and C. Ornelas; "The Structure-Property Relationship in Laponite Materials: From Weigner Glasses to Strong Self-Healing Hydrogels Formed by Non-Covalent Interactions," *Soft Matter*, **15**, 1278–1289 (2019)

Chen, M. H., L. L. Wang, J. J. Chung, Y. H. Kim, P. Atluri and J. A. Burdick; "Methods to Assess Shear-Thinning Hydrogels for Application as Injectable Biomaterials," *ACS Biomater. Sci. Eng.*, **3**, 3146–3160 (2017)

Chhabra, R. P. and J. F. Richardson; Non-Newtonian Flow and Applied Rheology: Engineering Applications, 2nd ed., pp. 111–114, Butterworth-Heinemann Press, Oxford, U.K. (1999)

Daly, A. C., L. Riley, T. Segura and J. A. Burdick; "Hydrogel Microparticles for Biomedical Applications," *Nat. Rev. Mater.*, **5**, 20–43 (2020)

Dávila, J. L. and M. A. d'Ávila; "Laponite as a Rheology Modifier of Alginate Solutions: Physical Gelation and Aging Evolution," *Carbohydr. Polym.*, **157**, 1–8 (2017)

Ewoldt, R. H., C. Clasen, A. E. Hosoi and G. H. McKinley; "Rheological Fingerprinting of Gastropod Pedal Mucus and Synthetic Complex Fluids for Biomimicking Adhesive Locomotion," *Soft Matter*, **3**, 634–643 (2007)

Gaharwar, A. K., N. A. Peppas and A. Khademhosseini; "Nanocomposite Hydrogels for Biomedical Applications," *Biotechnol. Bioeng.*, **111**, 441–453 (2014)

Gutowski, I. A., D. Lee, J. R. de Bruyn and B. J. Frisken; "Scaling and Mesostructure of Carbopol Dispersions," *Rheol. Acta*, **51**, 441–450 (2012)

Highley, C. B., C. B. Rodell and J. A. Burdick; "Direct 3D Printing of Shear-Thinning Hydrogels into Self-Healing Hydrogels," *Adv. Mater.*, **27**, 5075–5079 (2015)

Hirose, R., T. Nakaya, Y. Naito, T. Daidoji, O. Dohi, N. Yoshida, H. Yasuda, H. Konishi and Y. Itoh; "Identification of the Critical Viscoelastic Factor in the Performance of Submucosal Injection Materials," *Mater. Sci. Eng. C Mater. Biol. Appl.*, **94**, 909–919 (2019)

Hozumi, T., S. Ohta and T. Ito; "Analysis of the Calcium Alginate Gelation Process Using a Kenics Static Mixer," *Ind. Eng. Chem. Res.*, **54**, 2099–2107 (2015)

Hozumi, T., A. M. Sreedevi, S. Ohta and T. Ito; "Nonlinear Pressure Drop Oscillations during Gelation in a Kenics Static Mixer," *Ind. Eng. Chem. Res.*, **59**, 4533–4541 (2020)

Ito, T., Y. Yeo, C. B. Highley, E. Bellas, C. A. Benitez and D. S. Kohane; "The Prevention of Peritoneal Adhesions by in Situ Cross-Linking Hydrogels of Hyaluronic Acid and Cellulose Derivatives," *Biomaterials*, **28**, 975–983 (2007)

Khutoryanskiy, V. V.; "Advances in Mucoadhesion and Mucoadhesive polymers," *Macromol. Biosci.*, **11**, 748–764 (2011)

Li, Y., J. Rodrigues and H. Tomás; "Injectable and Biodegradable Hydrogels: Gelation, Biodegradation and Biomedical Applications," *Chem. Soc. Rev.*, **41**, 2193–2221 (2012)

Lokhande, G., J. K. Carrow, T. Thakur, J. R. Xavier, M. Parani, K. J. Bayless and A. K. Gaharwar; "Nanoengineered Injectable Hydrogels for Wound Healing Application," *Acta Biomater.*, **70**, 35–47 (2018)

Maeng, J. H., B. W. Bang, E. Lee, J. Kim, H. G. Kim, D. H. Lee and S. G. Yang; "Endoscopic Application of EGF-Chitosan Hydrogel for Precipitated Healing of GI Peptic Ulcers and Mucosectomy-Induced Ulcers," *J. Mater. Sci. Mater. Med.*, **25**, 573–582 (2014)

Mandal, A., J. R. Clegg, A. C. Anselmo and S. Mitragotri; "Hydrogels in the Clinic," *Bioeng. Transl. Med.*, **5**, e10158 (2020)

Nakagawa, Y., S. Ohta, M. Nakamura and T. Ito; "3D Inkjet Printing of Star Block Copolymer Hydrogels Cross-Linked Using Various Metallic Ions," *RSC Advances*, **7**, 55571–55576 (2017)

Nelson, A. Z. and R. H. Ewoldt; "Design of Yield-Stress Fluids: A Rheology-to-Structure Inverse Problem," *Soft Matter*, **13**, 7578–7594 (2017)

Nelson, A. Z., R. E. Bras, J. Liu and R. H. Ewoldt; "Extending Yield-Stress Fluid Paradigms," *J. Rheol. (N.Y.N.Y.)*, **62**, 357–369 (2018)

Nelson, A. Z., K. S. Schweizer, B. M. Rauzan, R. G. Nuzzo, J. Vermant and R. H. Ewoldt; "Designing and Transforming Yield-Stress Fluids," *Curr. Opin. Solid State Mater. Sci.*, **23**, 100758 (2019)

Norton, I. T., D. M. Goodall, S. A. Frangou, E. R. Morris and D. A. Rees; "Mechanism and Dynamics of Conformational Ordering in Xanthan Polysaccharide," *J. Mol. Biol.*, **175**, 371–394 (1984)

Ohta, S., S. Hiramoto, Y. Amano, S. Emoto, H. Yamaguchi, H. Ishigami, J. Kitayama and T. Ito; "Intraperitoneal Delivery of Cisplatin via a Hyaluronan-Based Nanogel/In Situ Cross-Linkable Hydrogel Hybrid System for Peritoneal Dissemination of Gastric Cancer," *Mol. Pharm.*, **14**, 3105–3113 (2017)

Onuma, W., S. Tomono, S. Miyamoto, G. Fujii, T. Hamoya, K. Fujimoto, N. Miyoshi, F. Fukai, K. Wakabayashi and M. Mutoh; "Irsogladine Maleate, a Gastric Mucosal Protectant, Suppresses Intestinal Polyp Development in *Apc*-Mutant Mice," *Oncotarget*, **7**, 8640–8652 (2016)

Pang, Y., J. Liu, Z. L. Moussa, J. E. Collins, S. McDonnell, A. M. Hayward, K. Jajoo, R. Langer and G. Traverso; "Endoscopically Injectable Shear-Thinning Hydrogels Facilitating Polyp Removal," *Adv. Sci. (Weinh)*, **6**, 1901041 (2019)

Pioche, M., M. Camus, J. Rivory, S. Leblanc, I. Lienhart, M. Barret, S. Chaussade, J. C. Saurin, F. Prat and T. Ponchon; "A Self-Assembling Matrix-Forming Gel Can Be Easily and Safely Applied to Prevent Delayed Bleeding after Endoscopic Resections," *Endosc. Int. Open*, 0**4**, E415–E419 (2016)

Rao, K. V. R. and P. Buri; "A Novel in Situ Method to Test Polymers and Coated Microparticles for Bioadhesion," *Int. J. Pharm.*, **52**, 265–270 (1989)

Ribeiro, A., M. M. Blokzijil, R. Levato, C. W. Visser, M. Castilho, W. E. Hennink, T. Vermonden and J. Malda; "Assessing Bioink Shape Fidelity to Aid Material Development in 3D Bioprinting," *Biofabrication*, **10**, 014102–014117 (2017)

Rutgeerts, P., E. Rauws, P. Wara, P. Swain, A. Hoos, E. Solleder, J. Halttunen, G. Dobrilla, G. Richter and R. Prassler; "Randomised Trial of Single and Repeated Fibrin Glue Compared with Injection of Polidocanol in Treatment of Bleeding Peptic Ulcer," *Lancet*, **350**, 692–696 (1997)

Song, K. W., Y. S. Kim and G. S. Chang; "Rheology of Concentrated Xanthan Gum Solutions: Steady Shear Flow Behavior," *Fibers Polym.*, **7**, 129–138 (2006)

Steele, A. N., L. M. Stapleton, J. M. Fary, H. J. Lucian, M. J. Paulsen, A. Eskandari, C. E. Hironaka, A. D. Thakore, H. Wang, A. C. Yu, D. Chan, E. A. Appel and Y. J. Woo; "A Biocompatible Therapeutic Catheter-Deliverable Hydrogel for *in situ* Tissue Engineering," *Adv. Healthc. Mater.*, **8**, 1801147 (2019)

Tsuji, Y., K. Ohata, T. Gunji, M. Shozushima, J. Hamanaka, A. Ohno, T. Ito, N. Yamamichi, M. Fujishiro, N. Matsuhashi and K. Koike; "Endoscopic Tissue Shielding Method with Polyglycolic Acid Sheets and Fibrin Glue to Cover Wounds after Colorectal Endo-

scopic Submucosal Dissection (with Video)," *Gastrointest. Endosc.*, **79**, 151–155 (2014)

Varadarajulu, S., S. Banerjee, B. A. Barth, D. J. Desilets, V. Kaul, S. R. Kethu, M. C. Pedrosa, P. R. Pfau, L. J. Tokar, A. Wang, L.-M. Wong K. Song and S. A. Rodriguez; "GI Endoscopes," *Gastrointest. Endosc.*, **74**, 1–6 (2011)

Vo, A., M. Doumit and G. Rockwell; "The Biomechanics and Optimization of the Needle-Syringe System for Injecting Triamcinolone Acetonide into Keloids," *J. Med. Eng.*, **2016**, 5162394 (2016)

Wahlberg, B., H. Ghuman, J. R. Liu and M. Modo; "*Ex vivo* Biomechanical Characterization of Syringe-Needle Ejections for Intracerebral Cell Delivery," *Sci. Rep.*, **8**, 9194 (2018)

Yan, C., M. E. Mackay, K. Czymmek, R. P. Nagarkar, J. P. Schneider and D. J. Pochan; "Injectable Solid Peptide Hydrogel as a Cell Carrier: Effects of Shear Flow on Hydrogels and Cell Payload," *Langmuir*, **28**, 6076–6087 (2012)

Yoshida, T., R. Hirose, Y. Naito, K. Inoue, O. Dohi, N. Yoshida, K. Kamada, K. Uchiyama, T. Ishikawa, T. Takagi, H. Konishi, T. Nakaya and Y. Itoh; "Viscosity: An Important Factor in Predicting the Performance of Submucosal Injection Materials," *Mater. Des.*, **195**, 109008 (2020)